Published OnlineFirst May 10, 2018; DOI: 10.1158/0008-5472.CAN-17-2676

Molecular Cell Biology

Cancer Research

R-spondin3 Is Associated with Basal-Progenitor Behavior in Normal and Tumor Mammary Cells

Johanna M. Tocci[1], Carla M. Felcher[1], Martín E. García Solá[1], María Victoria Goddio[1], María Noel Zimberlin[1], Natalia Rubinstein[1,2], Anabella Srebrow[1,2], Omar A. Coso[1,2], Martín C. Abba[3], Roberto P. Meiss[4], and Edith C. Kordon[1,5]

Abstract

R-spondin3 (RSPO3) is a member of a family of secreted proteins that enhance Wnt signaling pathways in diverse processes, including cancer. However, the role of RSPO3 in mammary gland and breast cancer development remains unclear. In this study, we show that RSPO3 is expressed in the basal stem cell–enriched compartment of normal mouse mammary glands but is absent from committed mature luminal cells in which exogenous RSPO3 impairs lactogenic differentiation. RSPO3 knockdown in basal-like mouse mammary tumor cells reduced canonical Wnt signaling, epithelial-to-mesenchymal transition-like features, migration capacity, and tumor formation *in vivo*. Conversely, RSPO3 overexpression, which was associated with some LGR and RUNX factors, highly correlated with the basal-like subtype among patients with breast cancer. Thus, we identified RSPO3 as a novel key modulator of breast cancer development and a potential target for treatment of basal-like breast cancers.

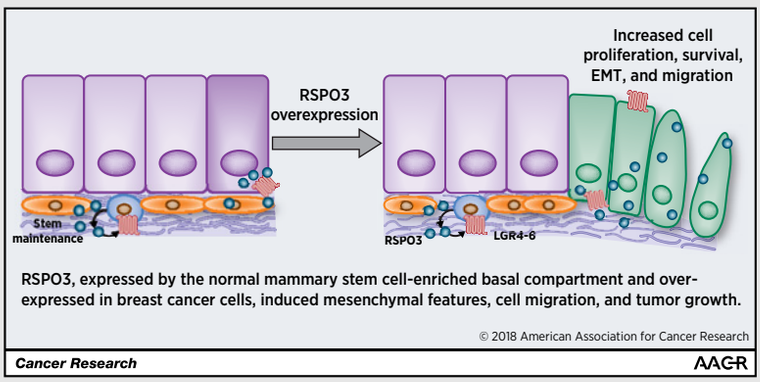

Significance: These findings identify RSPO3 as a potential therapetuic target in basal-like breast cancers.

Graphical Abstract: http://cancerres.aacrjournals.org/content/canres/78/16/4497/F1.large.jpg. *Cancer Res; 78(16); 4497–511.* ©2018 AACR.

Introduction

R-spondins (*roof plate-specific spondins;* RSPO) represent a group of four secreted proteins (RSPO1–4) that have been described in vertebrates. All four RSPOs have similar domain structures with two amino-terminal furin-like repeats and a thrombospondin domain situated toward the basic amino acid–rich carboxyl terminal domain, which can bind matrix glycosaminoglycans and/or proteoglycans (1). RSPOs potently enhance both canonical, through β-catenin activation, and noncanonical *Wnt* signaling pathways (2–4). At the cell membrane, secreted RSPOs simultaneously bind to leucine-rich repeat-containing G-protein–coupled receptors 4, 5, or 6 (LGR4–6; refs. 5, 6) and to extracellular domains of two membrane-bound E3 ubiquitin ligases, zinc and RING finger 3/RING finger 43 (ZNRF3/RNF43). This ternary complex, LGR–RSPO–ZNRF3/RNF43, induces autoubiquitination and membrane clearance of ZNRF3/RNF43, allowing the WNT receptor, Frizzled (FZD), to accumulate and enhance the activation of *Wnt* pathways (7).

WNT ligands activate canonical *Wnt* signaling by binding to FZD receptor, inducing the release of β-catenin from a cytosolic destruction multiprotein complex and its translocation to the nucleus, where it acts as a coactivator of the TCF/LEF family of transcription factors, promoting target gene transcription. This signaling pathway is essential to several

[1]CONICET-Universidad de Buenos Aires, Instituto de Fisiología, Biología Molecular y Neurociencias (IFIBYNE), Buenos Aires, Argentina. [2]Departamento de Fisiología, Biología Molecular y Celular, Universidad de Buenos Aires, Facultad de Ciencias Exactas y Naturales, Buenos Aires, Argentina. [3]Basic and Applied Immunological Research Center, School of Medicine, National University of La Plata, La Plata, Argentina. [4]Department of Pathology, Institute of Oncology Studies, National Academy of Medicine, Buenos Aires, Argentina. [5]Facultad de Ciencias Exactas y Naturales, Departamento de Química Biológica, Universidad de Buenos Aires, Buenos Aires, Argentina.

Note: Supplementary data for this article are available at Cancer Research Online (http://cancerres.aacrjournals.org/).

Corresponding Author: Edith C. Kordon, IFIByNE-UBA-CONICET, Facultad de Ciencias Exactas y Naturales, Universidad de Buenos Aires, IFIBYNE, Ciudad Universitaria, Buenos Aires 1428, Argentina. Phone: 5411-4576-3368; Fax: 5411-4576-3321; E-mail: ekordon@qb.fcen.uba.ar

doi: 10.1158/0008-5472.CAN-17-2676

Published OnlineFirst May 10, 2018; DOI: 10.1158/0008-5472.CAN-17-2676

developmental processes by regulation of cell proliferation, differentiation, and migration, whilst its deregulation underlies a wide range of pathologies including cancer (8).

The mammary gland undergoes most of its development postnatally, progressing through a series of developmental cycles regulated by systemic hormones and local factors (9, 10). The mammary epithelium is composed of luminal and basal compartments, surrounded by adipocytes and other stromal cells. The basal compartment consists of myoepithelial cells with contractile capacity and WNT-responsive mammary stem cells (MaSC; ref. 11) that reconstitute the gland upon transplantation into cleared mammary fat pads of host syngeneic mice (12). Importantly, LGRs have been recently described as MaSC markers and are WNT-regulated target genes (13, 14). Moreover, canonical *Wnt* signaling plays a critical role in controlling the enormous tissue expansion and remodeling during mammary gland development (15) through the maintenance and differentiation of MaSCs (16) and is implicated in breast carcinogenesis (17).

Due to their *Wnt* pathway–potentiating activity, RSPOs play critical roles in embryonic development and organogenesis as well as in the self-renewal and maintenance of stem cells in some adult tissues (1). Likewise, genomic rearrangements and transcriptional activation that result in elevated RSPO expression have been recently identified in mouse and human tumors, suggesting RSPOs may be functionally relevant for tumor development (18–20). Particularly, RSPO3 promotes angiogenesis and vasculogenesis (21, 22), several steps during embryogenesis (4), and represents a potent intestinal stem cell factor (23). Acting through canonical and noncanonical *Wnt* pathway activation, RSPO3 has been recently implicated in several cancer models, including colorectal, ovarian, and lung cancers (24, 25).

Several years ago, mouse mammary tumor virus (MMTV) insertions that promoted *Rspo3* overexpression were identified (26, 27). However, the role of RSPO3 in breast cancer and normal mammary gland development remains unclear. Here, we show that RSPO3 is expressed in the basal stem cell–enriched compartment of the mouse mammary gland. In mammary tumor cells, its overexpression is associated with the maintenance of mesenchymal-like features, migration capacity, and *in vivo* tumorigenesis. Moreover, we found that RSPO3 is associated with the basal-like human breast cancer subtype, which lacks efficient therapeutic options.

Materials and Methods

Cell culture, transfections, and differentiation procedures

The following mouse mammary cell lines, obtained directly from their originating laboratories or from American Type Culture Collection (ATCC), were used in this study: HC11 and EpH4 (Dr. Bernd Groner, Georg-Speyer-Haus, Frankfurt, Germany), LM3 (Dr. Elisa Bal, Institute of Oncology Ángel H. Roffo, Buenos Aires, Argentina), NMuMG (ATCC), SCg6 and SCp2 (Dr. Mina Bissell, Lawrence Berkeley National Laboratory, Berkeley, CA), and LM38-LP (Dr. Laura Todaro; Institute of Oncology Ángel H. Roffo; ref. 28). Because no mouse STR DNA fingerprinting analysis is available for them to date, no authentication was performed (see Supplementary Material for culture and differentiation procedures). SCg6 cells were stably transfected with pGIPZ/tGFP/shScrambled/puromycin or with different shRNA sequences of pGIPZ/tGFP/shRSPO3/puromycin (Thermo Scientific), and resistant clones were selected with 2 μg/mL puromycin (Sigma Aldrich) for 4 weeks. For epithelial-to-mesenchymal transition (EMT) assay, NMuMG cells were incubated with 60 ng/mL recombinant RSPO3 protein (rRSPO3; R&D Systems) or 2 ng/mL TGFβ (Sigma Aldrich) at indicated times. All cell lines used in this study were maintained in culture for 4 to 5 weeks, regularly monitored for mycoplasma contamination by PCR using specific primers and discarded in case of positive results.

RT-qPCR

Total RNA was isolated using TriReagent (MRC) according to the manufacturer's instructions. For RT, 250 ng or 1 μg RNA from sorted mouse mammary cell populations or cell cultures, respectively, were used. All qPCRs were performed using SYBR Green (Roche) and Stratagene Mx3000P System (Agilent Technologies). Gene expression levels were normalized to *Actinb1*, *Gapdh*, or *Hsp90ab1* as reference genes using the standard curve method. See Supplementary Material for more details and primer sequences.

Protein analysis

Total proteins were extracted in RIPA buffer and used for Western blotting. Blocked membranes were incubated with primary and secondary antibodies as follows: pAKT and AKT (Cell Signaling Technology; 4060S and 9272, respectively), E-cadherin (Thermo Scientific; 13-1900; ECCD2 clone), p-JNK, JNK, β-actin, and GAPDH (SCBT; sc-6254, sc-474, sc-1616, and sc-20357, respectively), RSPO3 (R&D Systems; MAB41201), vimentin (Abcam; 7783-500), IgG anti-mouse, anti-rabbit, or anti-rat (SCBT; sc-2005, sc-2004, and sc-2032, respectively). More details are given in Supplementary Material.

Conditioned media

To obtain conditioned media (CM), cells were cultured in supplemented medium for 24 hours that was replaced with serum-free medium for another 24 or 48 hours, as indicated. CMs were collected, precipitated overnight at −20°C with acetone, and centrifuged at 1,500 × *g* and 4°C for 20 minutes. Pellets were resuspended in 40 μL PBS containing SDS sample buffer and used for Western blotting. For competitive assay, cells were incubated with increasing concentrations of $KClO_3$ (Sigma Aldrich) in serum-free medium prior to CM collection.

Wound healing assay

Confluent monolayers were wounded with a pipette tip, cell debris was removed by washing with warm medium, and cells were cultured for 15 hours in serum-free medium. Images were captured using an Olympus SP-350 digital camera mounted on a microscope after wounding ($t = 0$ hour) and 15 hours later. Analysis was performed using Image-Pro-Plus software, and wound sizes in experimental monolayers were expressed relatively to controls.

β-Catenin transcriptional activity

Cells were transfected with 1 μg/well of pGL3-OT (TOP-Flash-like, TCF-LEF/β-catenin reporter), and pCMVLacZ as a control. Transfections were performed using polyethylenimine (Polysciences) according to the manufacturer's instructions. Cell extracts were prepared 48 or 72 hours later, using Reporter Lysis Buffer (Promega). Luciferase pGL3-OT activity was normalized to pCMVLacZ β-galactosidase activity. See Supplementary Material for detailed data.

Published OnlineFirst May 10, 2018; DOI: 10.1158/0008-5472.CAN-17-2676

Immunofluorescence

Fixed cells or 5-μm paraffin sections of mammary glands from 12-week-old mice were incubated with F-actin probe Rhodamine Phalloidin (Sigma Aldrich), anti-αSMA (Abcam, ab21027), anti–β-catenin (BD; #610154), anti-ERα (SCBT; sc-542), anti-Fibronectin (Sigma; F6140; clone FN-3E2), anti-RSPO3 (Sigma Aldrich; HPA029957), or anti-vimentin (Abcam; 7783-500) antibodies followed by incubation with Alexa Fluor 555 goat anti–mouse IgG, 647 donkey anti-mouse IgG, 488 donkey anti-goat IgG, and 647 donkey anti–rabbit IgG (Life Technologies). Cells were also stained with DAPI (Roche). Slides were examined under an Olympus FV100 confocal microscope, and images were analyzed with MacBiophotonics ImageJ. See Supplementary Material for more details.

Animals

Virgin female mice from C57BL/6 and BALB/c strains were maintained in a specific pathogen-free facility at the FCEN-UBA-CONICET, at constant temperature and humidity with a 12-hours light cycle. Animals were allowed food and water *ad libitum*. Mouse experiments were approved by local IACUC authorities and complied with regulatory standards of animal ethics.

Cell isolation and fluorescence-activated cell sorting

Lymph node–free mammary glands from 12-week-old virgin C57BL/6 mice were minced and digested to obtain single-cell suspensions prior flow cytometry analysis. See Supplementary Material for more details. For FACS, 5×10^5 cells from mouse single-cell suspensions were stained with fluorophore-conjugated antibodies (BioLegend). Specifically, cells were stained with anti-mouse CD31/CD140a/TER119/CD45-PE (Lineage cocktail; clones 145-2C11, RB6-8C5, M1/70, RA3-6B2, and Ter-119), anti-hamster IgG/anti-rat IgG2b/anti-rat IgG2a as lineage cocktail isotype controls, anti-mouse CD24-APC (clone M1/69), or anti-mouse CD29-FITC, for 30 minutes on ice in 10% (v/v) FBS/PBS. Stained populations were analyzed and sorted on a BD FACS Aria (II) Cell Sorting System (BD). Data acquisition and analysis were performed using FACS Diva software (BD).

In vivo studies

Six-week-old virgin BALB/c female mice were injected subcutaneously into the right ventral flank or within the right fourth mammary fat pad with 4×10^5 SCg6-shRspo3 or SCg6-shControl cells in 100 μL DMEM-F12 (8 mice per group; $n = 3$). Alternatively, 20-day-old BALB/c female mice were subjected to standard mammary fat pad clearing and then injected with the same amount of the indicated cells within the #4 cleared fat pads. Tumor measurements were carried out blindly with a caliper twice per week, and volumes were calculated using the formula $V = \pi/6 \times \text{length} \times (\text{width})^2$. Mice were euthanized when they met the institutional criteria for tumor size and overall health condition. Tumors were fixed in PBS-buffered 4% (v/v) formalin solution and embedded in paraffin. Lung experimental metastasis was induced by injecting 7×10^5 cells in 100 μLPBS through the tail vein. Up to 4 weeks after injection, animals were euthanized and their lungs were fixed via tracheal instillation of 4% (v/v) buffered formalin prior to removal. Paraffin-embedded lung samples were stained with hematoxylin and eosin (H&E) and entirely scanned. Metastatic regions in H&E-stained lungs were quantified by a metastasis area index, calculated as the ratio of metastasis to total lung areas.

Immunohistochemistry

IHC analysis was performed on 5-μm paraffin sections either of mammary glands from 12-week-old mice, mouse tumors and lung samples, or human mammary tissues with the Vectastain Elite ABC HRP Kit (Vector Laboratories) according to the manufacturer's instructions. Primary antibodies used were as follows: αSMA (Thermo Fisher Scientific, #RB-9010), cleaved caspase-3 (CC3; Cell Signaling Technology; 9661), ERα (SCBT; sc-542), Ki67 (Abcam; ab15580), KRT-14 (Thermo Fisher Scientific; #RB-9020), RSPO3 (Sigma Aldrich; HPA029957), SOX2 (Cell Signaling Technology; 3728), or vimentin (Abcam; 7783-500). For CC3 and Ki67 quantification, cells were counted at 1,000× (5 fields per section at least; 1,000 cells per field) excluding boundaries and necrotic regions; $n = 3$.

Human mammary tissues

Tissue microarray (TMA) of breast cancers was purchased from US Biomax (#BR1505b). Paraffin-embedded breast tissue specimens were acquired from hospitals associated with the School of Medical Sciences, National University of La Plata, Argentina, after obtaining written informed consents from patients (according to the Declaration of Helsinki, 2000) and the approval by the Institutional Review Board.

In silico analysis

Comparative analysis of *RSPO3*, *CDH1*, *FN1*, *VIM*, *SNAI1*, *SNAI2*, and *TWIST* gene expression was performed in 51 breast normal and cancer cell lines obtained from three independent studies (GSE10843, GSE12777, and GSE41445). Expression profiles were developed using the Affymetrix HG-U133 Plus2 platform (GPL570). Mouse *Rspo3* mRNA expression was analyzed among luminal cells isolated from the mammary glands of adult female mice derived from the GSE47377 dataset obtained from GEO2R resource. Visualization and statistical analysis of RSPO3 expression were done with R/Bioconductor. Comparative analysis of *RSPO3*, *LGR4–6*, *RUNX1–3* mRNA expression profiles across 1097 primary human breast carcinomas was performed using The Cancer Genome Atlas (TCGA) Network breast cancer project. Correlation analysis was done with Pearson test using corrplot R package. Profiles were also compared according to PAM50-intrinsic subtypes and ESTIMATE (Estimation of Stromal and Immune Cells in Malignant Tumors using Expression data) scores. Comparative analysis of *RSPO3*, *ER*/*PR*/*HER2*, and *CDH1*/*VIM*/*SNAI2*/*TWIST* mRNA expression among 1985 breast cancer samples was done using the METABRIC dataset. Kruskal–Wallis and χ^2 were used as statistic tests. See Supplementary Material for more details.

Statistical analyses

Statistical significance of differences was evaluated using the software GraphPad Prism5. Data are presented as mean ± SEM unless otherwise noted.

Results

RSPO3 is expressed in distinct mouse and human mammary cell lines

In order to assess whether *Rspo3* is expressed in mammary cells in the absence of MMTV infection, we performed an *in silico RSPO3* mRNA profiling analysis in a set of 51 human breast normal and cancer cell lines. Obtained values revealed

Published OnlineFirst May 10, 2018; DOI: 10.1158/0008-5472.CAN-17-2676

that breast cancer cells express high levels of *RSPO3* as compared with the nontumorigenic cell line MCF-10A. Interestingly, among tumor cells, *RSPO3* mRNA levels resulted higher in basal-like (ER^-PR^-) than in luminal-like (ER^+PR^+) breast cancer cell lines (BCCL). Notably, a subset of basal ER^-PR^- cells (i.e., MDA-MB-436, HCC1143, BT549, HDQP1, and Hs578t), which are characterized by low expression of epithelial cell–cell adhesion and luminal differentiation markers, as well as by high expression of genes involved in EMT and cancer stem cell (CSC) features (29), showed the highest level of *RSPO3* expression (Fig. 1A and B; Supplementary Fig. S1). Besides, we determined a significant correlation of *RSPO3* with some of those markers, such as *CDH1*, *VIM*, and *TWIST1* (Fig. 1C and D). In addition, analysis of mouse mammary tumors also revealed that ER^- cells (LM38-LP and SCg6) express higher levels of *Rspo3* than ER^+ tumor cells (C4-derived, MPA-induced tumors, see Supplementary Material; Fig. 1E). Among nontumor cell lines (HC11, EpH4, and SCp2), we found that *Rspo3* mRNA levels were associated with vimentin expression, a broadly used basal/mesenchymal marker, and that proliferating HC11 cells showed the highest *Rspo3* levels (Fig. 1E). This cell line produces its own extracellular matrix and resembles mammary stem/progenitor cells in the proliferating undifferentiated stage, exhibiting pluripotent capacity and expression of proteins associated with mesenchymal phenotype (30). Importantly, as these cells reached lactogenic differentiation, *Rspo3* expression significantly decreased, similarly to vimentin levels (Fig. 1E).

At the protein level, it was determined that RSPO3 is secreted to the extracellular space, as it was detected in the CM of cultured mammary tumor cells (Fig. 1F). Our results also confirmed that, once secreted, RSPO3 may strongly interact with membrane-associated and/or extracellular matrix heparan sulfate proteoglycans, because the addition of potassium chlorate, an inhibitor of sulfation, increased RSPO3 levels in the CM of mammary tumor cells (Fig. 1G).

RSPO3 is differentially expressed in stromal and basal mammary subpopulations

To determine whether RSPO3 is constitutively expressed in the normal mouse mammary gland, studies using IHC were carried out. RSPO3 cytoplasmic staining was detected in a subset of basal epithelial cells and within the stroma. Figure 2A shows its localization as well as the distribution of basal myoepithelial markers cytokeratin 14 (KRT14) and α-smooth-muscle actin (α-SMA), and the MaSC marker SOX2 (14) on serial mammary sections. Noteworthy, RSPO3 localization was clearly different from the luminal marker, estrogen receptor-α (ERα; Fig. 2A and B), and coimmunofluorescent studies also revealed accumulation of RSPO3 surrounding α-SMA–positive cells (Fig. 2B).

To identify the specific subpopulations expressing *Rspo3*, we examined its mRNA level in FACS-purified luminal ($Lin^-CD24^{hi}CD29^+$), MaSC-enriched basal ($Lin^-CD24^+CD29^{hi}$) epithelial and stromal ($Lin^-CD24^-CD29^+$) populations (Fig. 2C). The successful separation was confirmed by *Krt18* (luminal), *Krt14* (basal), and *Vim* (basal/stromal) marker expression analysis (Fig. 2D). We found that *Rspo3* was predominantly expressed in stromal cells and in the MaSC-enriched basal epithelial fraction. Interestingly, in the mammary epithelial compartment, we observed that *Rspo3* levels displayed a similar distribution as its putative receptor, the basal MaSC marker, *Lgr4* (Fig. 2D; ref. 14). Collectively, these data demonstrate that RSPO3 is expressed in normal mammary glands of adult virgin female mice both in the stem cell–enriched basal epithelial and stromal populations, whereas it is absent from committed luminal epithelial cells.

RSPO3 is associated with basal phenotype in mammary cells

As indicated above (Fig. 1E), *Rspo3* levels decrease as HC11 cells reach lactogenic differentiation in culture. In addition, *in silico* analysis revealed that the committed alveolar luminal cell population of mid-pregnant animals expresses lower levels of *Rspo3* than alveolar luminal stem/progenitor mammary cells of virgin mice (Fig. 3A). Moreover, we determined that recombinant RSPO3 (rRSPO3) protein significantly reduced β-casein expression levels in luminal-like, functionally normal SCp2 and EpH4 cells under lactogenic conditions (Fig. 3B). To further investigate whether RSPO3 could alter mammary epithelial phenotype, we cultured NMuMG cells with rRSPO3 protein. It was observed that rRSPO3 induced canonical Wnt pathway activation (Supplementary Fig. S2A) and promoted the acquisition of fibroblast-like, mesenchymal morphology, similar to that obtained with transforming growth factor-β (TGFβ; Fig. 3C). We detected a significantly increased expression of the mesenchymal markers fibronectin and vimentin, and a reduced expression of the epithelial marker E-cadherin by RT-qPCR and/or Western blot analysis (Fig. 3D and E). Similar results were obtained in SCp2 cells after rRSPO3 treatment (Supplementary Fig. S2B). Taken together, these results suggest that RSPO3 could play a relevant role in the normal mammary gland biology, promoting the maintenance of an uncommitted basal-like mammary epithelial phenotype and inducing EMT-like and CSC features, which may be the underlying mechanisms for transforming breast cancer cells that overexpress RSPO3.

To validate the involvement of RSPO3 in the malignant phenotype of basal cancer cells, the SCg6 cell line, which expresses high levels of *Rspo3* (Fig. 1E), was stably transfected with a scrambled shRNA (shControl) or with four different *Rspo3* shRNA sequences. Two clones (#2A and #4B) displaying a knockdown (KD) efficiency of ∼50% at mRNA and protein levels were selected for further studies (Fig. 4A; Supplementary Fig. S3A). Rspo3-KD cells showed a change in cell morphology from spread-out, mesenchymal-like to cobblestone, epithelial-like cells when cultured up to confluence (Fig. 4B). Although subtler, cell shape differences were also detected at subconfluence (Supplementary Fig. S3B). Consistently, F-actin was predominantly reorganized into cortical bundles associated with cell–cell adhesions in Rspo3-KD cells in contrast to the F-actin assembled into thick parallel bundles, or actin stress fibers, in shControl cells (Fig. 4C). Moreover, an increase in membrane-bound β-catenin levels, as a key component of cell–cell adhesion, was obtained in Rspo3-KD cells as compared with stabilized-cytoplasmic β-catenin displayed by shControl cells (Fig. 4D). Although E-cadherin expression remained undetectable, analysis of basal/mesenchymal markers revealed a reduction of vimentin and fibronectin levels in Rspo3-KD cells, as compared with shControl cells (Fig. 4E and F). We also determined that the morphological change observed in Rspo3-KD cells was accompanied by a significant decrease in migration capacity (Fig. 4G).

Published OnlineFirst May 10, 2018; DOI: 10.1158/0008-5472.CAN-17-2676

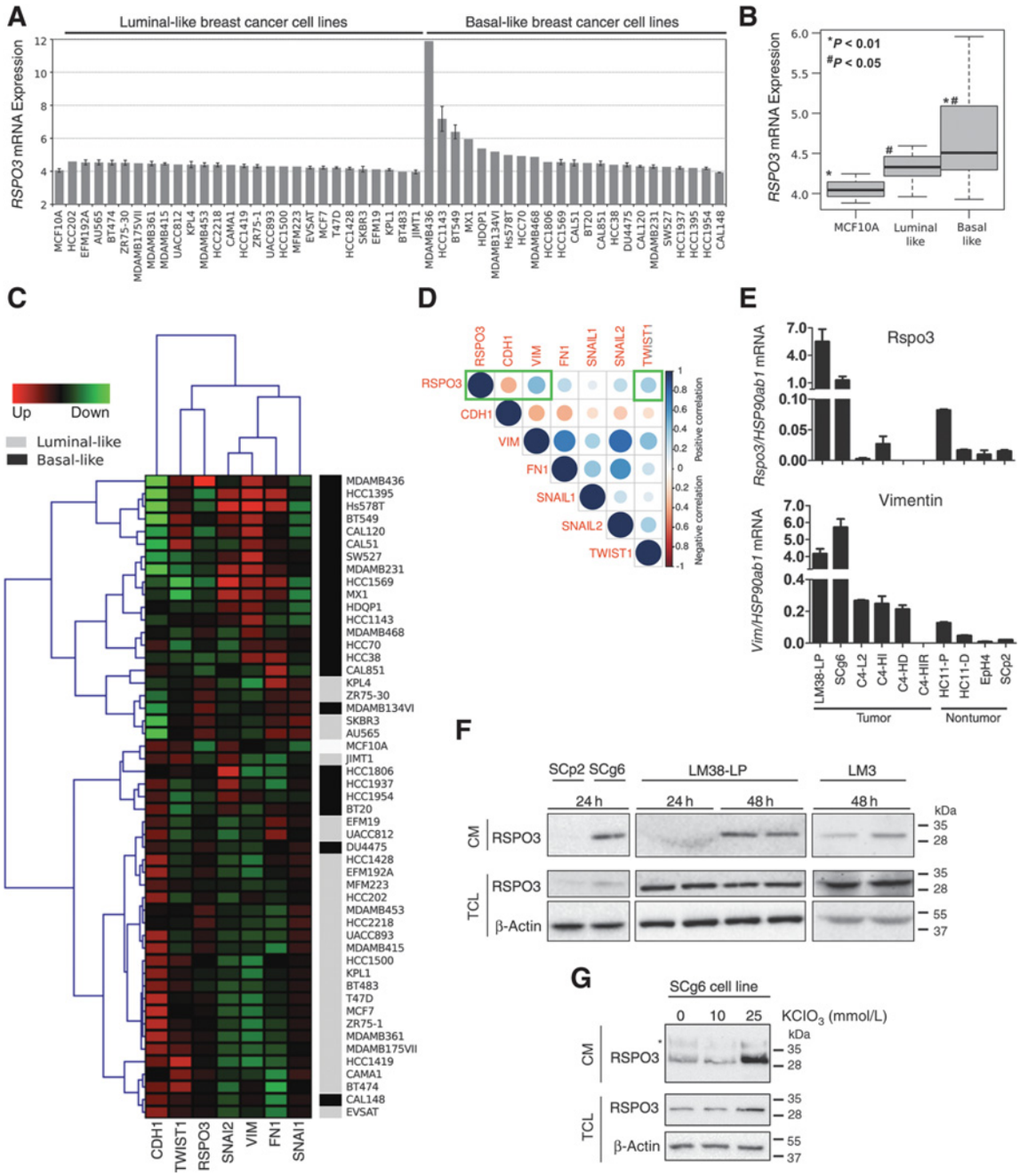

Figure 1.

RSPO3 is expressed in human and mouse mammary cancer cell lines. **A,** *RSPO3* mRNA expression profile based on a compiled *in silico* dataset of 50 human BCCLs: 27 luminal-like and 23 basal-like BCCLs, and the nontumorigenic MCF-10A cell line, obtained from the GSE10843, GSE12777, and GSE41445 datasets. **B,** Box plot of *RSPO3* mRNA expression between nontumor, luminal-like and basal-like BCCLs from the compiled dataset, showing statistically significant differences between groups. **C** and **D,** Hierarchical clustering analysis (**C**) and correlation matrix (**D**) of *RSPO3, CDH1, VIM, FN1, SNAI1, SNAI2*, and *TWIST* among breast cancer cell lines using the same datasets as in **A**. Green squares in **D** show genes with statistically significant differences; $P < 0.01$. **E,** RT-qPCR analysis of *Rspo3* mRNA expression levels and the basal/mesenchymal marker vimentin (*Vim*) in tumor (LM38-LP, SCg6, C4-L2, C4-HI, C4HD, and C4-HIR) and nontumor (HC11, SCp2, and EpH4) mouse mammary cells. Analysis of *Rspo3* expression in HC11 cells was performed during proliferative stem-like (HC11-P) and lactogenic differentiation (HC11-D) stages. Expression data were normalized by *HSP90ab1* mRNA. Error bars, SEM ($n = 3$). **F,** Representative Western blot analysis of RSPO3 levels in serum-free conditioned media (CM) and total cell lysates (TCL) of indicated mouse mammary cell lines. LM3, $ER^{-}PR^{-}$ mouse mammary tumor cell line. Cells were cultured in serum-free medium for 24 or 48 hours prior to harvesting. β-Actin was used as a loading control. **G,** Representative Western blot analysis of RSPO3 levels in total cell lysates and serum-free conditioned media of SCg6 cells incubated with increasing concentrations (0–25 mmol/L) of potassium chlorate ($KClO_3$), an inhibitor of sulfation. β-Actin was used as a loading control. *, high-molecular-weight band of RSPO3, possibly due to posttranslational modifications.

Published OnlineFirst May 10, 2018; DOI: 10.1158/0008-5472.CAN-17-2676

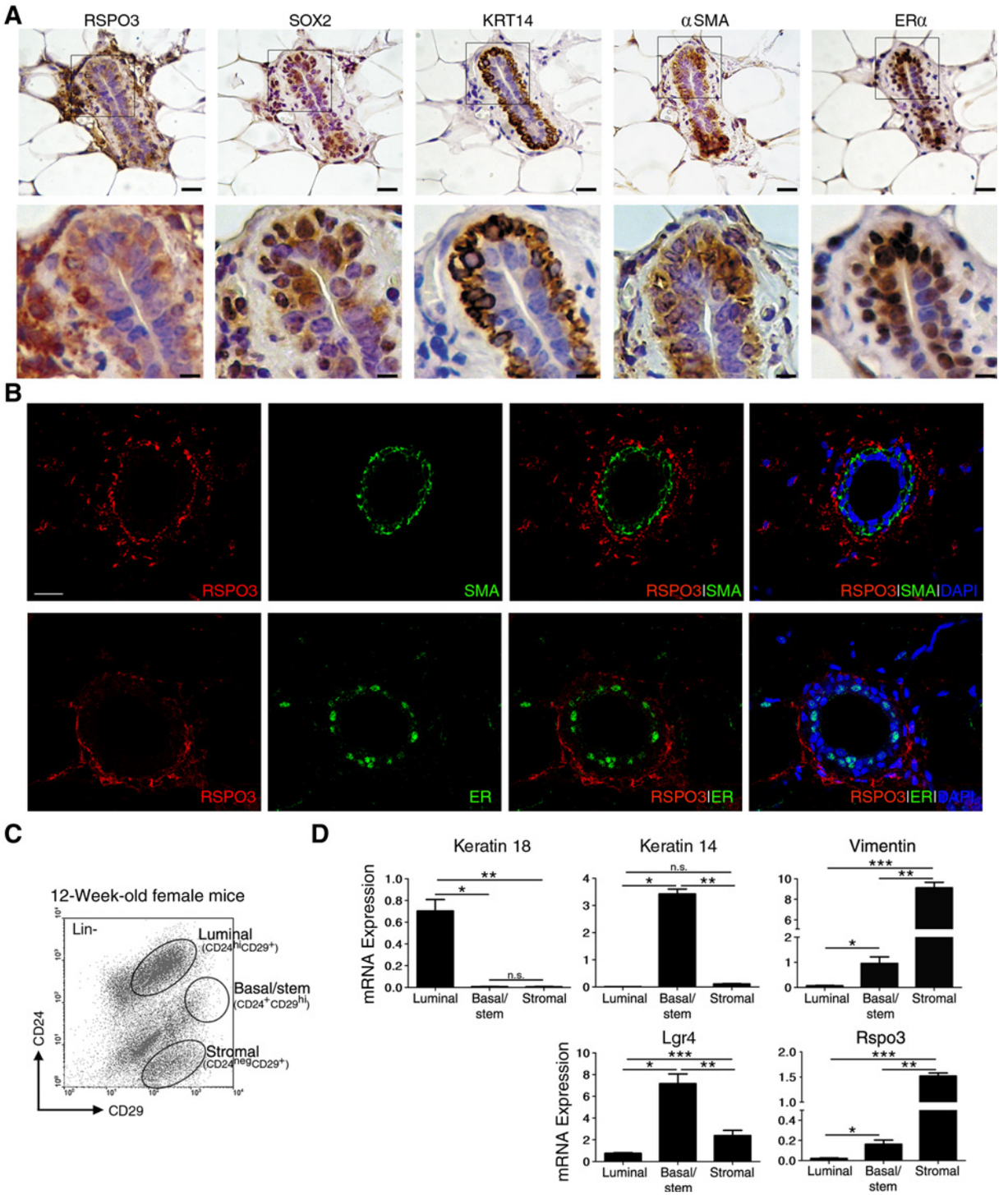

Figure 2.

Rspo3 is expressed in the stroma and stem cell–enriched basal mammary epithelial cell subpopulations. **A,** Immunohistochemical staining of serial mouse mammary sections with antibodies specific to RSPO3 and to stem (SOX2), basal (cytokeratin 14, KRT14, and α-SMA), and luminal (ERα) lineage markers. Bottom, higher magnification of top images. Scale bars, 50 μm and 17 μm, respectively. **B,** Representative micrographs of coimmunofluorescence assays showing RSPO3 (red), α-SMA (green; top), and ERα (green; bottom), in mouse mammary sections; DAPI (blue), nuclei. Scale bars, 50 μm. **C,** FACS segregation of lineage-negative (Lin; CD31, CD45, Ter119) mammary cells into luminal ($CD24^{hi}CD29^{+}$), stem cell–enriched basal ($CD24^{+}CD29^{hi}$), and stromal ($CD24^{-}CD29^{+}$) subpopulations. A representative FACS dot plot is shown. **D,** RT-qPCR analysis of luminal cytokeratin 18 (*Krt18*), basal *Krt14*, stem *Lgr4*, mesenchymal *Vim* markers, and *Rspo3* expression in luminal, basal/stem, and stromal FACS-sorted subpopulations normalized to *HSP90ab1*. Data represent mean ± SEM of three replicate experiments; Tukey test following one-way ANOVA. *, **, ***, $P < 0.05$; n.s., not significant. All experiments were performed using 12-week-old virgin female mice.

Published OnlineFirst May 10, 2018; DOI: 10.1158/0008-5472.CAN-17-2676

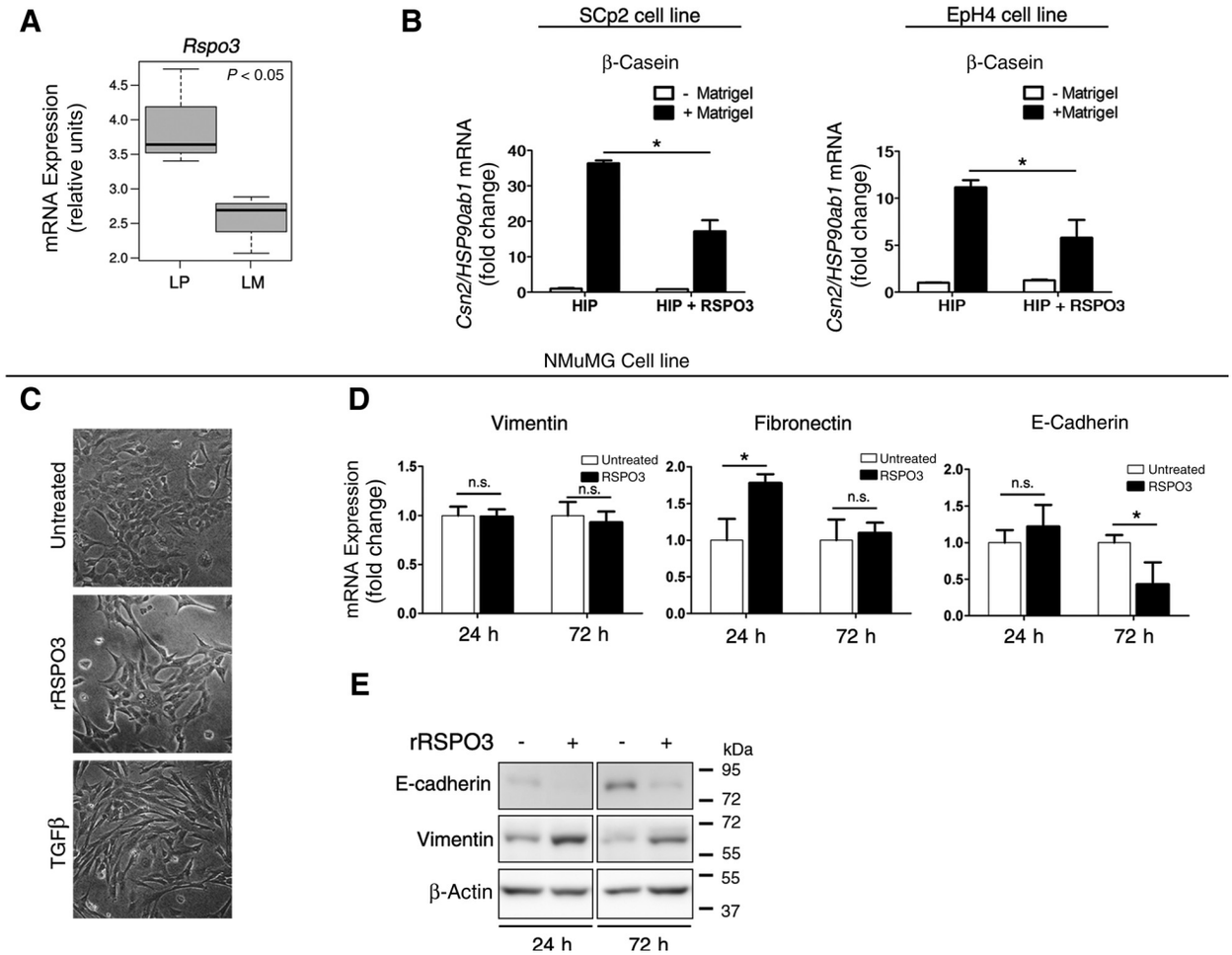

Figure 3.

RSPO3 inhibits lactogenic differentiation and promotes mesenchymal/basal phenotype in mouse mammary epithelial cells. **A,** *Rspo3* mRNA expression determined by oligo-microarray analysis (probe 1443187_at) obtained from GSE47377 GEO Superserie of alveolar epithelial cells: luminal progenitors (LP) and luminal mature at mid-gestation (LM), isolated from the mammary glands of adult virgin female mice. **B,** Quantitative expression analysis of the β-casein gene. Mouse mammary luminal-like SCp2 and EpH4 cells were cultured in the presence of lactogenic hormones, with or without 1.5% v/v laminin-rich basement membrane (Matrigel) to promote lactogenic differentiation and with or without rRSPO3 (60 ng/mL) for 72 hours. Total RNA was isolated and subjected to RT-qPCR. **C,** Representative micrographs showing morphological changes induced in NMuMG cells 24 hours after treatment with rRSPO3 protein (60 ng/mL) or TGFβ (2 ng/mL) as an EMT-positive control. **D,** RT-qPCR analysis of mesenchymal (vimentin and fibronectin) and epithelial (E-cadherin) markers in NMuMG cells treated or not with rRSPO3 protein during 24 and 72 hours. Gene expression data were normalized to *HSP90ab1* mRNA and is shown as fold change (mean ± SEM) relative to untreated cells. **E,** Representative Western blot analysis of EMT-associated markers in NMuMG cells 24 and 72 hours after treatment with rRSPO3. β-Actin was used as a loading control. Experiments **B–E** were performed in triplicate. Student *t* test, *, $P < 0.05$; n.s., not significant.

Then, we investigated the signaling pathway underlying RSPO3 activity in tumor basal mammary cells. While no changes in JNK phosphorylation levels were found (Supplementary Fig. S3C), as a noncanonical *Wnt* pathway activation marker, Rspo3-KD cells displayed a significant reduction of canonical *Wnt* pathway activation, because less nuclear β-catenin activity was detected by reporter gene expression (Fig. 4H). In addition, Rspo3-KD cells exhibited a reduction in AKT phosphorylation levels (Supplementary Fig. S3D), in agreement with several reports showing the role of the phosphoinositide 3-kinase (PI3K)/AKT pathway in enhancing the canonical *Wnt* pathway during normal mammary gland development and tumorigenesis (31). Taken together, these results suggest that RSPO3 could be relevant for breast cancer progression, favoring the maintenance of a migratory basal/mesenchymal-like phenotype possibly through canonical *Wnt* pathway activation and a cross-talk with the PI3K/AKT cascade.

Rspo3-KD reduces *in vivo* tumor growth and metastasis in basal mammary cancer cells

To determine the effect of knocking down *Rspo3* on tumor growth *in vivo*, Rspo3-KD and shControl SCg6 cells were subcutaneously injected into female mice. It was determined that shControl-derived tumors appeared earlier and grew faster than those obtained from Rspo3-KD cells. Nine days after cell injection, all shControl-derived tumors were palpable and had

Published OnlineFirst May 10, 2018; DOI: 10.1158/0008-5472.CAN-17-2676

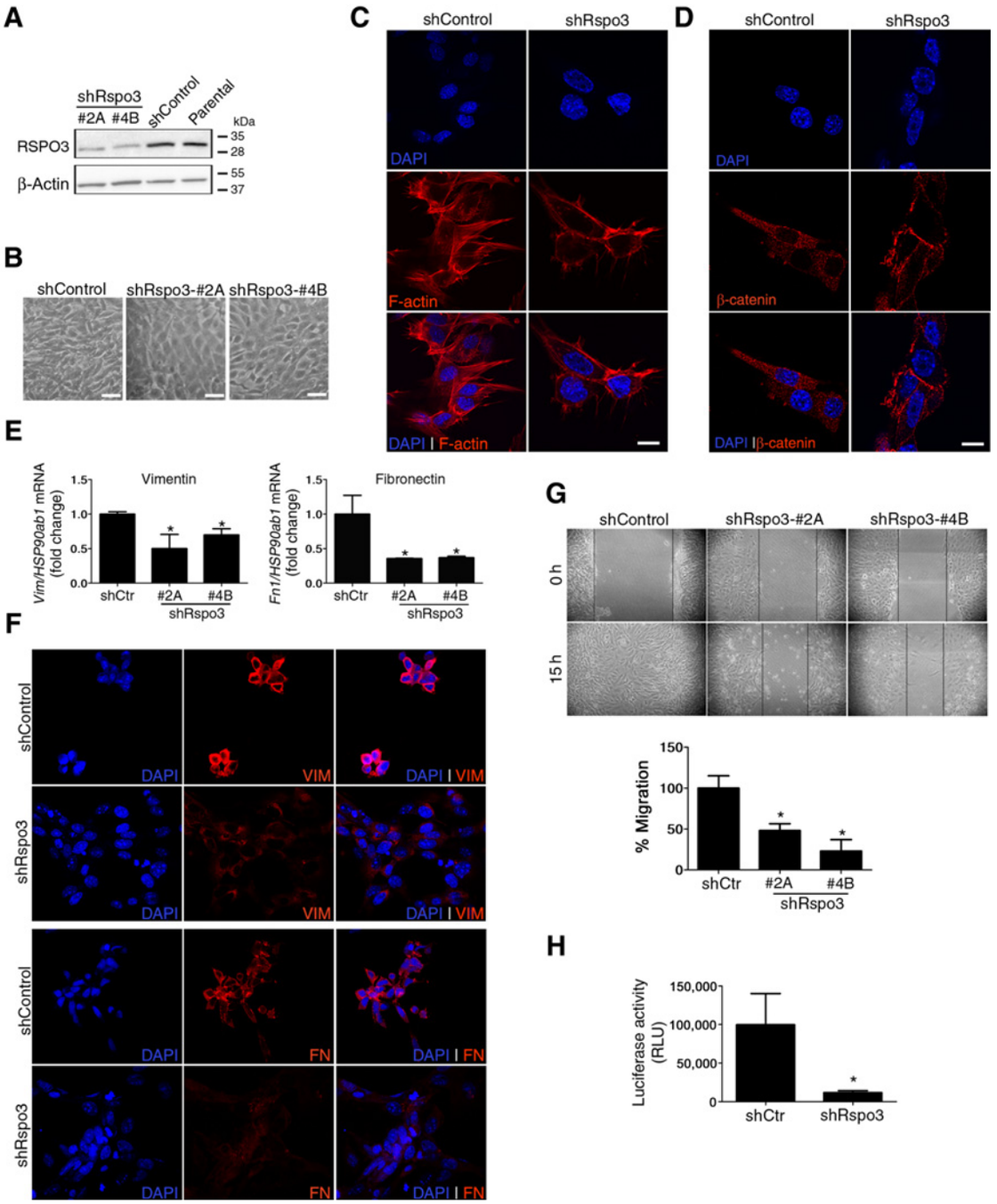

Figure 4.

Rspo3 downregulation alters basal phenotype in tumor SCg6 mammary cells. **A,** Western blot analysis of RSPO3 levels in SCg6 cells either naïve (parental) or stably transfected with a scrambled shRNA (shControl) or with shRNA sequences targeting *Rspo3* (shRspo3). 2A and 4B represent two different isolated clones. **B,** Representative micrographs of confluent shRspo3 (2A and 4B) and shControl cells. Original magnification, ×200. **C** and **D,** Representative micrographs of immunocytochemistry assays showing F-actin (red) and β-catenin (red), respectively, in stably transfected shRspo3 (clone 4B) or shControl SCg6 cells; DAPI (blue), nuclei. Scale bars, 10 μm. **E,** RT-qPCR analysis of basal/mesenchymal markers, vimentin and fibronectin, in shRspo3 and shControl cells. Gene expression data were normalized to *HSP90ab1* mRNA and are shown as fold change (mean ± SEM) relative to shControl cells. Experiments were performed in triplicate and Dunnett test following one-way ANOVA was performed. *, $P < 0.05$. **F,** Representative micrographs of immunocytochemistry assays showing vimentin (red; top) and fibronectin (red; bottom) in stably transfected shRspo3 (clone 4B) or shControl SCg6 cells; DAPI (blue), nuclei. **G,** Representative images of wound healing assays performed with SCg6 cells, with a graph showing the quantitation of cell migration ($n = 4$; *, $P < 0.05$ indicates statistically significant differences versus shControl migration; Dunnett test following one-way ANOVA). **H,** shRspo3 and shControl cells were transiently transfected with luciferase β-catenin reporter and β-galactosidase (normalizing transfection control) vectors. The reporter activity was measured 48 hours after transfection. Error bars, SD ($n = 4$). Student *t* test; *, $P < 0.05$.

Published OnlineFirst May 10, 2018; DOI: 10.1158/0008-5472.CAN-17-2676

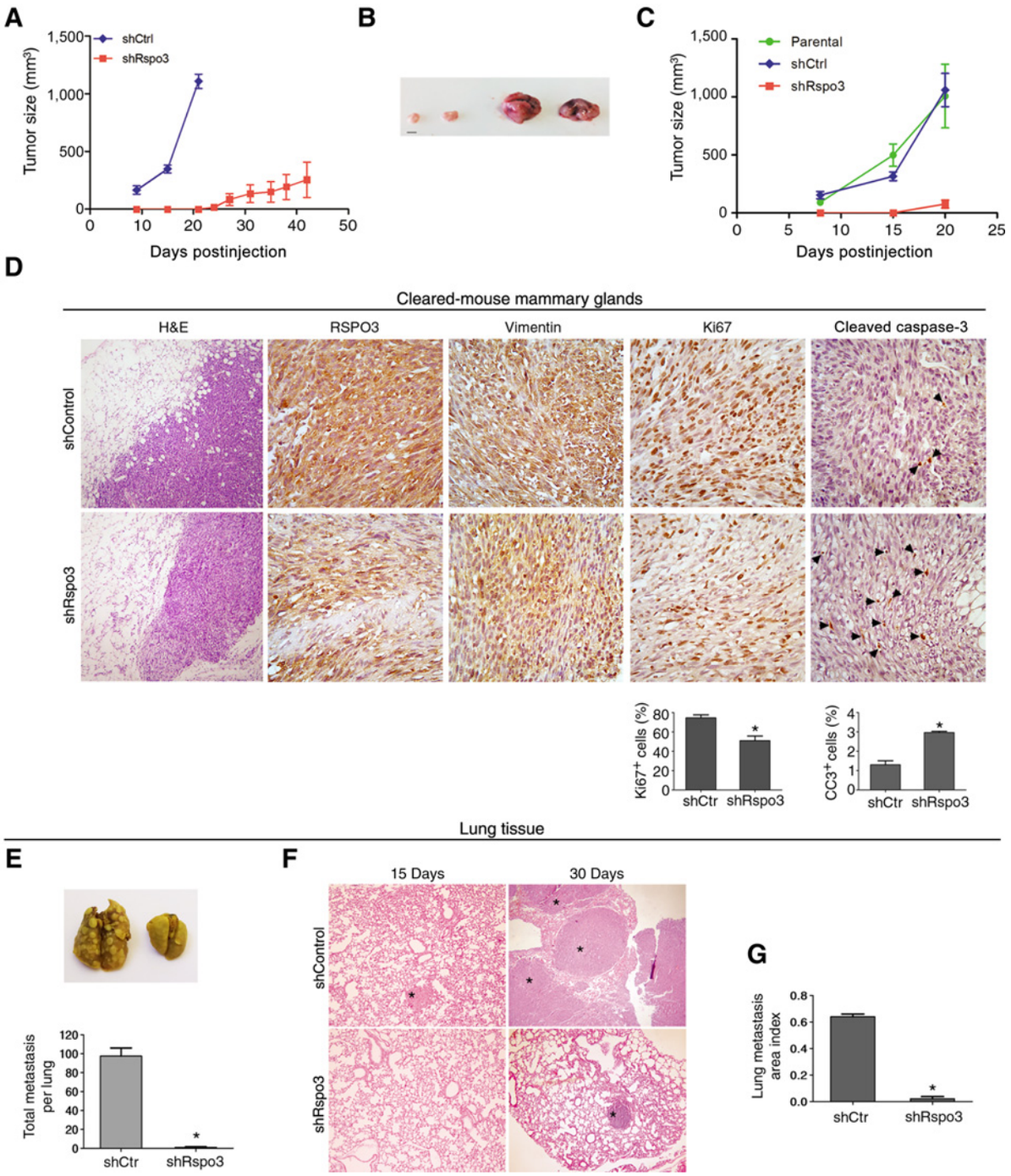

Figure 5.

Rspo3 downregulation in SCg6 cells reduces tumor growth and metastasis *in vivo*. **A,** Tumor growth of shRspo3 (clone: 4B) and shControl cells implanted subcutaneously. Tumors were measured with a caliper starting 9 days after inoculation, when the tumors became detectable under the skin. Their volumes were calculated using the formula $\pi/6 \times a \times b^2$, where a is the longest dimension of the tumor and b is the width. **B,** Representative image of intramammary shRspo3-4B and shControl tumors isolated from mice 20 days after injection (scale bar, 50 mm). **C,** Tumor growth of shRspo3 (clone: 4B) and shControl cells implanted into #4 mammary fat pad (day = 0) BALB/c females. **D,** Representative micrographs showing H&E (original magnification, ×100) and RSPO3, vimentin, Ki67, and CC3 IHC (original magnification, ×400) in shRspo3-4B and shControl tumors obtained after cell inoculation into cleared fat pads. Arrowheads, CC3-positive cells. Quantification of Ki67 and CC3-positive cells is shown in bottom graphs. Student *t* test; *, $P < 0.05$. **E,** Representative image and macrometastasis quantification of excised lungs 30 days after tail-vein inoculation of shRspo3-4B and shControl cells. $n = 3$. **F,** Representative micrographs of H&E staining of lung tissue invaded by shRspo3-4B and shControl cells, 15 or 30 days after cell injection into the tail vein. *, mammary tumor cells; original magnification, ×100. **G,** Metastasis quantification by lung metastasis area index, 30 days after cell inoculation; $n = 3$.

Published OnlineFirst May 10, 2018; DOI: 10.1158/0008-5472.CAN-17-2676

to be euthanized 20 days after injection due to their tumor size. In contrast, tumors from Rspo3-KD cells appeared much later or did not show tumor development even after 60 days after inoculation (Fig. 5A). A similar study was performed inoculating parental, shControl and Rspo3-KD SCg6 cells into the #4 mammary fat pads, up to 20 days after injection to compare tumors at the same endpoint. Once again, tumors from Rspo3-KD cells arose later and were smaller than those derived from control cells (Fig. 5B and C). Histologic analysis revealed that both Rspo3-KD and shControl tumors expressed RSPO3 and were composed by undifferentiated spindle cells that invaded mammary fat tissue and entrapped host mammary ducts (Supplementary Fig. S4). In addition, when Rspo3-KD and shControl cells were transplanted into cleared fat pads, no differences to the previous approaches regarding tumor growth were detected. After 9 days, shControl tumors reached 69.9 ± 23.3 mm^3 and displayed invasive behavior toward the fatty stroma, while Rspo3-KD–derived tumors were barely palpable and looked encapsulated (H&E staining, Fig. 5D). Besides, Rspo3-KD implants displayed heterogeneous lower expression of RSPO3 and vimentin, as well as less Ki67-positive nuclei and a higher number of CC3-positive cells, compared with shControl tumors (Fig. 5D).

To determine whether RSPO3 also affects secondary tissue invasion, Rspo3-KD and shControl cells were injected into the tail vein of female mice. Fifteen days after injection, mice carrying shControl cells exhibited lung micrometastasis, which fully developed into macrometastasis that comprised the entire lungs 2 weeks later. In contrast, no tumor tissue was observed in lungs of mice carrying Rspo3-KD cells 15 days after inoculum, and in only one of them a single macrometastasis was found 30 days after injection (Fig. 5E). Besides, sequentially sliced lungs of mice inoculated with Rspo3-KD cells showed a significant reduction in the number of micrometastasis compared with controls (Fig. 5F and G). All together, these data demonstrate the relevance of RSPO3 for *in vivo* development of a basal mammary tumor model.

RSPO3 is overexpressed in human breast cancer and is associated with basal-like tumors

In order to assess *RSPO3* expression in human mammary tissue, IHC was performed on 21 samples of malignant and benign breast lesions. We found that most of these samples showed positive immunoreactivity for RSPO3 (62%; 13/21; Fig. 6A–D; Supplementary Table S1). Furthermore, RSPO3 was clearly detected in the basal compartment of differentiated ducts and lobules in neoplastic and nonneoplastic samples (Fig. 6E–H). RSPO3 expression was then analyzed by IHC in a TMA of 74 invasive ductal breast carcinoma cases. Notably, 70% (52/74) of tumors showed low to strong RSPO3-positive staining, while only 30% (22/74) resulted negative (z-test: $P < 0.001$; Fig. 6I–N). When RSPO3 score was compared with clinical and histopathologic parameters, neither clinical stage nor biomarker (ER/PR/Her2 and Ki67) expression exhibited a significant correlation with RSPO3 levels (Supplementary Tables S2–S4). However, the expression data of the TCGA breast cancer project from 1,985 human breast carcinomas revealed that *RSPO3* was highly expressed in triple-negative (TN) samples ($ER^-PR^-Her2^-$), compared with ER^+ subtypes ($ER^+PR^{+/-}Her2^{+/-}$; Fig. 7A), and showed significant *RSPO3* overexpression in the basal-like subtype (Fig. 7B). Moreover, by subdividing basal-like breast cancer category within the intrinsic subtypes, we determined significantly high *RSPO3* expression in claudin-low, basal-like tumors (Fig. 7C), which are characterized by low to absent expression of differentiated luminal cell markers, high enrichment for EMT markers, immune response genes, and CSC-like features (29). Besides, *RSPO3* mRNA levels were negatively correlated with epithelial markers, as E-cadherin, and positively with the EMT and CSC markers, vimentin, *SLUG*, and *TWIST*, in primary human breast tumors (Fig. 7D). Then, through the ESTIMATE method, we found that *RSPO3* expression was associated with elevated lymphocytic and stromal components (Fig. 7E), which are present in most basal-like breast cancers (32). Nevertheless, no significant association between *RSPO3* mRNA expression and lower overall survival was detected in patients with basal-like primary breast carcinomas (Supplementary Fig. S5A).

Finally, to propose RSPO3 as a relevant autocrine breast tumor factor, we analyze expression levels of certain factors previously shown to promote RSPOs expression and activity. *In silico* analysis revealed that among breast carcinomas, *RSPO3* is expressed in association with the three RSPO receptors, *LGR4–6* (Fig. 7F), and showed a positive correlation with the runt-related transcription factor (RUNX) family (Supplementary Fig. S5B) that may induce *Rspo3* expression in mammary tumor cells (33). Particularly, *RSPO3* levels significantly correlated with *LGR4–6* and *RUNX3* levels, among the members of these two families (Fig. 7G). Comparisons between different intrinsic molecular breast cancer subtypes revealed that these genes were also overexpressed in the basal-like subtype (Fig. 7H), consistently with *RSPO3* expression.

Discussion

Activation of the *Wnt* pathway has been described as a cell-biological program required for the correct development of the mammary gland (15), particularly promoting the maintenance and differentiation of MaSCs (16). RSPOs and LGR4–6 were recently found to constitute a ligand–receptor system with critical roles in normal development and stem cell survival through modulation of *Wnt* signaling in several tissues (5, 6). However, their roles in breast carcinogenesis have been less explored. Previously, we identified MMTV-promoted *Rspo3* upregulation (26), which led to mammary tumor formation in mice (27). We have also observed that 3T3 cells overexpressing *Rspo3* showed cell contact inhibition and anchorage-independent growth, which confirmed its pro-oncogenic capacity, as well as modulation of the AKT and JNK signaling pathways (Supplementary Fig. S6A–S6D).

Here, we show that *RSPO3* is overexpressed in human BCCLs compared with nontumor cells. Interestingly, the highest levels of *RSPO3* mRNA were found in a subset of basal-like BCCLs with a highly aggressive phenotype and EMT and CSC features (34). Consistently, established basal-like mouse mammary cell lines that exhibited high *Rspo3* levels also expressed vimentin, a basal/mesenchymal marker described as a target of canonical *Wnt* pathway activation promoting cell migration and invasion in human breast cells (35). The association between *Rspo3* and vimentin was also evident in the nontumorigenic mammary cell line HC11, because detectable levels of both mRNAs were found in the proliferative phase. Interestingly, proliferative undifferentiated HC11 cells are

Published OnlineFirst May 10, 2018; DOI: 10.1158/0008-5472.CAN-17-2676

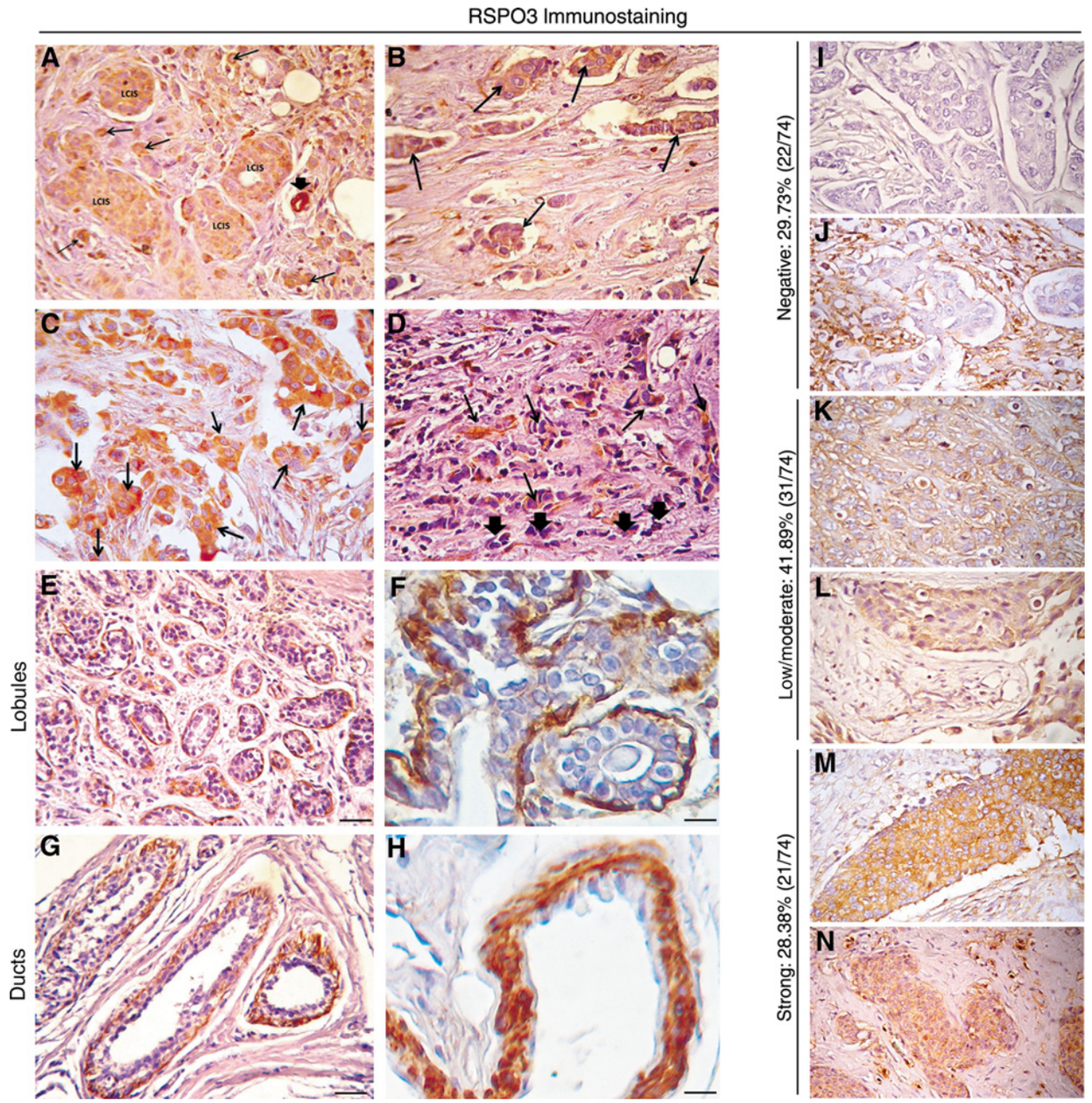

Figure 6.

RSPO3 is expressed in human breast cancer and in the basal compartment of nonneoplastic breast tissue. IHC studies were carried out on several breast samples. **A,** Lobular carcinoma *in situ* (LCIS) and stromal infiltrating cells (arrows) with moderate immunostaining and a small duct (arrowhead) with strong immunostaining for RSPO3. **B,** Infiltrating cords (arrows) of a ductal not otherwise specified (NOS) carcinoma with moderate immunostaining for RSPO3. **C,** Intense cytoplasmic immunostaining for RSPO3 in cells (arrows) of a ductal NOS carcinoma. **D,** Rows of infiltrating cells from a lobular carcinoma, some with moderate (arrows) and others with negative (arrowhead) immunostaining for RSPO3. Original magnification of **A–D,** ×400. **E–H,** Representative micrographs showing intense RSPO3 immunostaining in basal and myoepithelial cells of lobules and ducts from human hyperplastic breast sections; scale bar, left, 50 μm; scale bars, right, 100 μm. Original magnification of **E–H,** ×400. **I–N,** Representative tissue microarray micrographs of ductal invasive breast carcinoma samples showing infiltrating cords with cytoplasmic negative (**I–J**), low/moderate (**K–L**), or strong (**M–N**) RSPO3 immunostaining. In **J**, tumor tissue is surrounded by positive lymphocytes and fibroblasts. In **M,** some cells display a perinuclear reinforcement of RSPO3 expression. Original magnification of **I–M,** ×400. Percentages of cases with negative, low/moderate, and strong RSPO3 immunostaining are indicated for each of these categories.

considered stem-like cells due to their self-renewal and pluripotent capacity (30). In agreement with these observations, we determined that in mice *Rspo3* is expressed by the basal, stem cell–enriched mouse mammary compartment, associated with the expression of the RSPO receptor *Lgr4*. Likewise, RSPO3 was detected in the basal layer of neoplastic and nonneoplastic

Published OnlineFirst May 10, 2018; DOI: 10.1158/0008-5472.CAN-17-2676

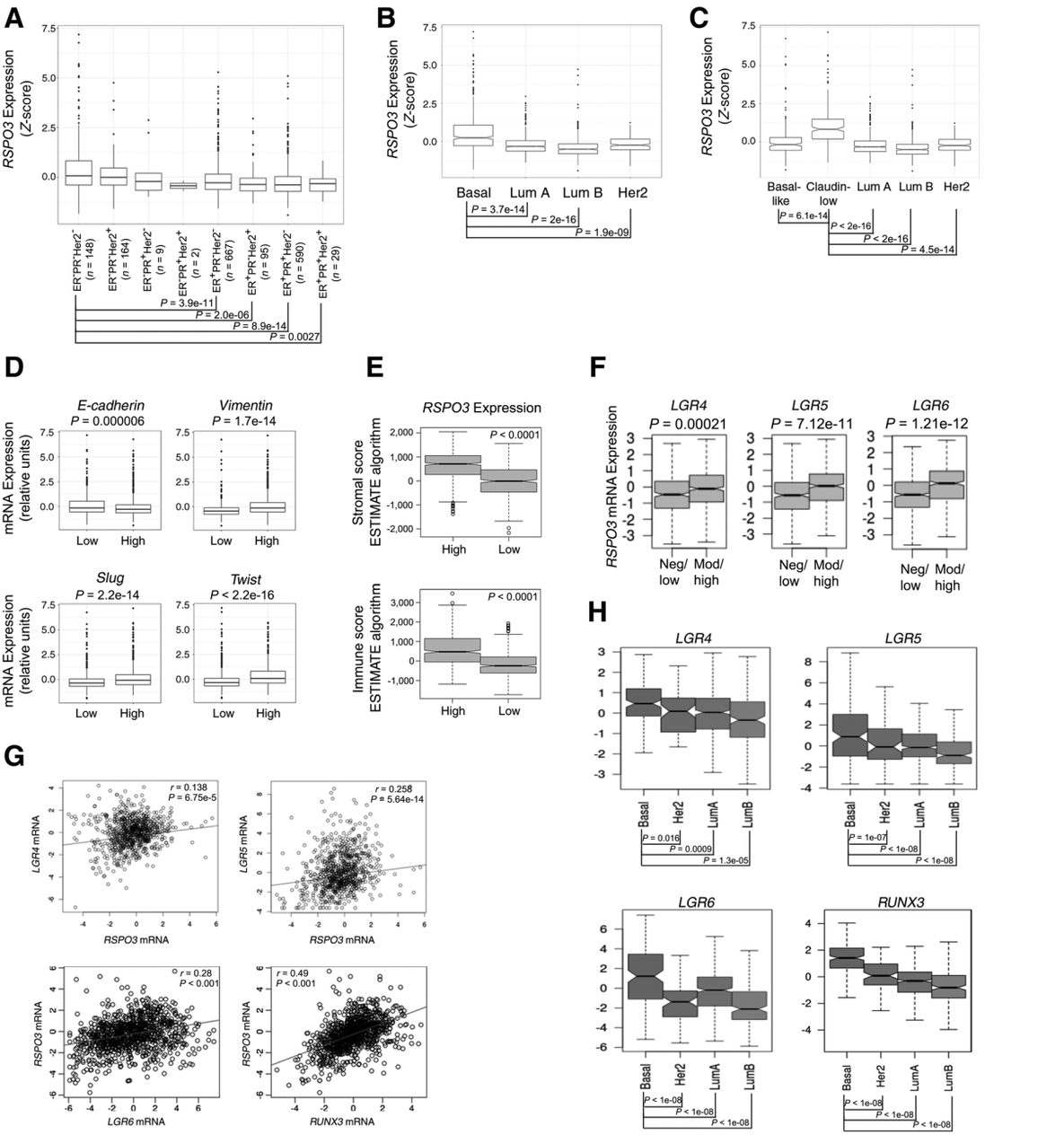

Figure 7.

Basal-like breast tumors show high expression of *RSPO3*. **A,** *RSPO3* expression levels according to ER, PR, and Her2 biomarker expression using *in silico* data mining of the TCGA cBioportal METABRIC database (1,985 samples). $ER^{-}PR^{-}Her2^{-}$ versus $ER^{-}PR^{-}Her2^{+}$, $ER^{-}PR^{+}Her2^{-}$, or $ER^{-}PR^{+}Her2^{+}$ resulted in not significant by pairwise comparisons using the Tukey and Kramer test. **B,** Comparative box plot analysis of *RSPO3* mRNA expression profiles according to intrinsic subtypes (luminal A, luminal B, Her2, and basal-like) among primary breast carcinomas, by pairwise comparisons using Tukey and Kramer test and the same TCGA's dataset as in **A**. Correlation analysis among normal and breast cancer samples was done using R/Bioconductor software. **C,** Comparative box plot analysis of *RSPO3* mRNA expression, according to intrinsic breast cancer subtypes, separating claudin-low subtype from basal-like category using the same TCGA's dataset as in **A**. **D,** Box plot expression analysis of *RSPO3* with respect to expression level of *CDH1* (E-cadherin), *VIM* (vimentin), *SNAI2* (Slug), and *TWIST*, as EMT markers, using the same TCGA's dataset as in **A**. Kruskal–Wallis χ^2 was used as statistic test. **E,** Box plot of *RSPO3* mRNA expression in association with stromal and immune scores using the ESTIMATE method in the TCGA breast cancer RNA-Seq dataset (1,097 primary breast carcinomas samples) obtained from the UCSC Xena Browser (https://xenabrowser.net). *RSPO3* mRNA expression was classified in high or low levels based on the StepMiner one-step algorithm. **F,** *RSPO3* mRNA levels in association with negative/low or moderate/high *LGR4–6* expression levels among the TCGA breast cancer RNA-Seq dataset as in **E**. **G,** Correlation analysis of *RSPO3* expression with mRNA levels of its putative receptors, *LGR4–6*, and a member of the transcription factor family of *RUNX* genes, *RUNX3*, in human breast samples using the TCGA breast cancer RNA-Seq dataset as in **E**. **H,** *LGR4–6* and *RUNX3* expression levels among the intrinsic breast cancer subtypes based on gene expression profiling, using the same the TCGA breast cancer RNA-Seq dataset as in **E**.

Published OnlineFirst May 10, 2018; DOI: 10.1158/0008-5472.CAN-17-2676

ducts in human glands. Thus, these findings suggest that RSPO3 might be playing a relevant role in *Wnt* pathway activation and MaSCs' maintenance. A similar role of RSPO3 has been described in the intestinal stem niche, where it enhances the activity of WNT ligands secreted by epithelial and stromal populations (23). In fact, inhibition of RSPO3 activity, using blocking antibodies in human colorectal tumor xenografts, reduces the expression of several tumor stem cell–associated genes, thereby linking the activity of RSPO3 to the maintenance of epithelial homeostasis and the tumorigenesis of that tissue through hyperactivation of stem cell genes (25). In addition, we showed that RSPO3, once secreted, remains bound to the extracellular matrix and/or face of the cell membrane, and therefore it may exert its activity on the same cell population. Moreover, we found that *Rspo3* expression decreased as HC11 cells reach lactogenic differentiation, whereas rRSPO3 reduced β-casein expression in differentiated luminal cells. Hence, our results suggest that RSPO3 would participate in maintaining the stem niche of the normal mammary gland, inhibiting differentiation of the luminal compartment.

We are not the first to find out that a member of the RSPO protein family is present in the normal mouse mammary gland. It has been demonstrated that *Rspo1* is expressed by luminal cells and, together with WNT4, mediates hormone action on MaSC expansion (36). We still do not know whether *Rspo3* expression in the gland is regulated during development. However, its presence in stromal and basal mammary cells suggests that RSPO3 would contribute to the maintenance of the MaSCs and/or the MaSC niche in the adult female mice, because it has been shown a similar distribution and biological role in the intestine (23). Moreover, as *RSPO1* mRNA levels resulted lower than *RSPO3* in basal-like breast cancers (Fig. 7B; Supplementary Fig. S7), we propose that RSPO3 would play a more significant role in the development of this breast cancer subtype.

Many extracellular factors and signaling pathways described in normal mammary gland development and tumorigenesis, such as the canonical *Wnt* pathway, are also involved in the process of EMT (37–39). In this study, we observed that RSPO3 caused the acquisition of a spindle-shaped phenotype, typical of cells that have lost their epithelial properties, together with the modulation of relevant EMT markers. Interestingly, it has been determined that certain features associated with a partial EMT are visible in nontumor conditions, playing an important role in adult tissue remodeling. For example, during normal mammary branching morphogenesis, EMT-related genes are expressed specifically in terminal end buds, inhibiting epithelial differentiation in favor of the acquisition of migratory features (40, 41). Therefore, the ability of RSPO3 to induce EMT-associated events might also be important for mammary gland development during puberty.

Our results also demonstrate that RSPO3 is relevant for the migratory basal/mesenchymal-like phenotype in mouse mammary tumor cells, possibly through canonical *Wnt* pathway activation and a cross-talk with the PI3K/AKT cascade. This conclusion is based on the following obtained evidence: (i) RSPO3 promoted the maintenance of a spindle-shaped morphology and the expression of CSC- and EMT-associated genes such as vimentin and fibronectin; (ii) RSPO3 increased the ability of basal tumor cells to migrate in culture and to grow and invade secondary tissues *in vivo*; (iii) RSPO3 enhances canonical *Wnt* pathway activation and AKT phosphorylation, interplay also observed by our group in *Rspo3*-overexpressing 3T3 cells. Collectively, these results are consistent with reports showing that canonical *Wnt* signaling blockage decreases migratory potential and growth in soft agar of basal-like breast cancer cells (42, 43) and that the cross-talk between β-catenin/*Wnt* and PI3K/AKT pathways plays a critical role in the regulation of normal and malignant stem/progenitor cells during mammary gland development and carcinogenesis (44, 45). Besides, our *in silico* analysis shows that *RSPO3* mRNA levels were associated with high expression of stem cell markers in tumors from patients with breast cancer. Therefore, RSPO3 might promote the transcription of stem cell–related genes during normal and neoplastic mammary development through activation of *Wnt*/AKT pathways. The long latency of shRspo3–SCg6 tumors indicates the relevance of this protein for *in vivo* tumor development. Because Claudin-low breast tumor cells show high expression of RSPO3, and this cancer subtype has been shown to be enriched in functional CSCs (46), we postulate that inhibiting expression of RSPO3 in SCg6 cells may decrease their cancer stem cell properties, reducing the capability of tumor grafting and growth *in vivo*. Therefore, the impact of altering RSPO3 levels on Wnt pathway activation, EMT, and migration capacity observed in culture would be associated with SCg6-cancer stem cell population ability for survival, grafting, and generation of the appropriate microenvironment for tumor implantation and development *in vivo*.

By IHC, we found that most tumor samples from 74 patients with breast cancer resulted positive for RSPO3, while no significant association between this protein and the levels of clinically relevant biomarkers was determined. However, RNA-Seq analysis of 1,985 human breast carcinomas from the TCGA breast cancer database revealed that *RSPO3* was highly expressed in TN samples, compared with ER^+ tumors, independently from their PR and Her2 levels, and in the basal-like subtype among the intrinsic categories (29). This cancer subtype is a heterogeneous breast cancer group with fewer therapeutic options than luminal tumors, because they lack ER/PR expression and $Her2/Neu^+$ amplification. Several studies have recently demonstrated a high cytoplasmic and nuclear accumulation of β-catenin in ∼60% of human breast cancers, particularly in TNs, associated with the expression of EMT-related genes (47) and a MaSC enrichment (48–50). These results, beyond relating the canonical *Wnt* pathway with a poor clinical prognosis, showed that this activation was not due to mutations in the β-catenin gene, highlighting the importance of studying new factors, such as RSPO3, that could enhance canonical *Wnt* pathway activation in the most aggressive forms of breast cancer. Interestingly, we determined a positive association of *RSPO3* with *LGR4–6* and *RUNX3*, which are also overrepresented in the basal subtype. Although a dual activity of *RUNX* genes in promoting or inhibiting breast cancer development has been established (51), the data shown herein are consistent with our recent report showing that RUNX1 activates the transcription of *Rspo3* in mouse mammary tumor cells (33). Therefore, we propose that deregulation of the RUNX family might also lead to *RSPO3* overexpression in human breast cancer. However, further studies will be required to dissect the exact mechanism of how the RUNX3–RSPO3–LGR axis functions to modulate *Wnt* signaling in TN breast cancers.

Within the basal category, we found a significantly higher expression of *RSPO3* in the claudin-low subtype. It has been shown that in both mice and humans, this subtype has the largest percentage of tumors in which the MaSC signature

Published OnlineFirst May 10, 2018; DOI: 10.1158/0008-5472.CAN-17-2676

predominates (52). However, given that these aggressive tumors exhibit EMT and CSCs features (29), they may originate from the luminal progenitor population prior to acquiring adult MaSC and/or mesenchymal properties (52). Therefore, we propose that in mouse and human mammary glands, *RSPO3* is expressed in the progenitor population, promoting their inherent stemness properties and preventing luminal differentiation. Eventually, *RSPO3* overexpression in progenitor cells or expression in the luminal compartment might lead to malignant transformation and transdifferentiation through a process driven by EMT inducers.

Finally, we suggest that RSPO3 might be a potential molecular target for the prevention and treatment of breast cancer, particularly the TN subtype. We hypothesize that blocking its activity might provide a new opportunity not only to reduce tumor bulk but also to deplete CSCs that initiate and promote metastatic spread and recurrence.

Disclosure of Potential Conflicts of Interest

No potential conflicts of interest were disclosed.

Authors' Contributions

Conception and design: J.M. Tocci, A. Srebrow, E.C. Kordon
Development of methodology: J.M. Tocci, C.M. Felcher, M.E. García Solá, M.V. Goddio, M.N. Zimberlin, E.C. Kordon
Acquisition of data (provided animals, acquired and managed patients, provided facilities, etc.): R.P. Meiss
Analysis and interpretation of data (e.g., statistical analysis, biostatistics, computational analysis): J.M. Tocci, M.E. García Solá, M.V. Goddio, N. Rubinstein, M.C. Abba, R.P. Meiss, E.C. Kordon
Writing, review, and/or revision of the manuscript: J.M. Tocci, N. Rubinstein, O.A. Coso, R.P. Meiss, E.C. Kordon
Administrative, technical, or material support (i.e., reporting or organizing data, constructing databases): J.M. Tocci
Study supervision: A. Srebrow, O.A. Coso, E.C. Kordon

Acknowledgments

This project has been supported by grant PICT 2014-0844 awarded by the National Agency of Scientific and Technological Promotion (ANPCyT), Argentina, to E.C. Kordon. The authors want to thank Amaranta Avendaño, Lirane Moutinho, and Mariela Veggetti for their excellent technical assistance; Mina Bissell, Elisa Bal de Kier Joffé, Laura Todaro, and Claudia Lanari for kindly providing cell lines or cell material to develop some of the experiments; Jorge Filmus for providing the pGL3-OT vector; and Ana Quaglino for her guidance in the differentiation assays. J.M. Tocci is indebted to the training provided by Dr. Cathrin Brisken and her team in mouse mammary FACS techniques.

The costs of publication of this article were defrayed in part by the payment of page charges. This article must therefore be hereby marked *advertisement* in accordance with 18 U.S.C. Section 1734 solely to indicate this fact.

Received September 5, 2017; revised March 9, 2018; accepted April 30, 2018; published first May 10, 2018.

References

1. de Lau WB, Snel B, Clevers HC. The R-spondin protein family. Genome Biol 2012;13:242.
2. Kamata T, Katsube K-i, Michikawa M, Yamada M, Takada S, Mizusawa H. R-spondin, a novel gene with thrombospondin type 1 domain, was expressed in the dorsal neural tube and affected in Wnts mutants. Biochim Biophys Acta 2004;1676:51–62.
3. Kazanskaya O, Glinka A, del Barco Barrantes I, Stannek P, Niehrs C, Wu W. R-Spondin2 is a secreted activator of Wnt/beta-catenin signaling and is required for Xenopus myogenesis. Dev Cell 2004;7:525–34.
4. Ohkawara B, Glinka A, Niehrs C. Rspo3 binds syndecan 4 and induces Wnt/PCP signaling via clathrin-mediated endocytosis to promote morphogenesis. Dev Cell 2011;20:303–14.
5. Carmon KS, Gong X, Lin Q, Thomas A, Liu Q. R-spondins function as ligands of the orphan receptors LGR4 and LGR5 to regulate Wnt/β-catenin signaling. Proc Natl Acad Sci U S A 2011;108:11452–7.
6. Glinka A, Dolde C, Kirsch N, Huang YL, Kazanskaya O, Ingelfinger D, et al. LGR4 and LGR5 are R-spondin receptors mediating Wnt/beta-catenin and Wnt/PCP signalling. EMBO Rep 2011;12:1055–61.
7. de Lau W, Peng WC, Gros P, Clevers H. The R-spondin/Lgr5/Rnf43 module: regulator of Wnt signal strength. Genes Dev 2014;28:305–16.
8. Clevers H, Nusse R. Wnt/beta-catenin signaling and disease. Cell 2012;149:1192–205.
9. Sternlicht MD. Key stages in mammary gland development: the cues that regulate ductal branching morphogenesis. Breast Cancer Res 2006;8:201.
10. Macias H, Hinck L. Mammary gland development. Wiley Interdiscip Rev Dev Biol 2012;1:533–57.
11. Zeng YA, Nusse R. Wnt proteins are self-renewing factors for mammary stem cells and promote their long-term expansion in vivo. Cell Stem Cell 2010;6:568–77.
12. Kordon EC, Smith GH. An entire functional mammary gland may comprise the progeny from a single cell. Development 1998;125:1921–30.
13. Plaks V, Brenot A, Lawson DA, Linnemann JR, Van Kappel EC, Wong KC, et al. Lgr5-expressing cells are sufficient and necessary for postnatal mammary gland organogenesis. Cell Rep 2013;3:70–8.
14. Wang Y, Dong J, Li D, Lai L, Siwko S, Li Y, et al. Lgr4 regulates mammary gland development and stem cell activity through the pluripotency transcription factor Sox2. Stem Cells 2013;31:1921–31.
15. Chu EY, Hens J, Andl T, Kairo A, Yamaguchi TP, Brisken C, et al. Canonical WNT signaling promotes mammary placode development and is essential for initiation of mammary gland morphogenesis. Development 2004;131:4819–29.
16. van Amerongen R, Bowman AN, Nusse R. Developmental stage and time dictate the fate of Wnt/beta-catenin-responsive stem cells in the mammary gland. Cell Stem Cell 2012;11:387–400.
17. Yu QC, Verheyen EM, Zeng YA. Mammary Development and Breast Cancer: A Wnt Perspective. Cancers (Basel) 2016;8:65.
18. Klauzinska M, Baljinnyam B, Raafat A, Rodriguez-Canales J, Strizzi L, Endo Greer Y, et al. Rspo2/Int7 regulates invasiveness and tumorigenic properties of mammary epithelial cells. J Cell Physiol 2012;227:1960–71.
19. Seshagiri S, Stawiski EW, Durinck S, Modrusan Z, Storm EE, Conboy CB, et al. Recurrent R-spondin fusions in colon cancer. Nature 2012;488:660–4.
20. Hao HX, Jiang X, Cong F. Control of Wnt receptor turnover by R-spondin-ZNRF3/RNF43 signaling module and its dysregulation in cancer. Cancers (Basel) 2016;8:54.
21. Kazanskaya O, Ohkawara B, Heroult M, Wu W, Maltry N, Augustin HG, et al. The Wnt signaling regulator R-spondin 3 promotes angioblast and vascular development. Development 2008;135:3655–64.
22. Scholz B, Korn C, Wojtarowicz J, Mogler C, Augustin I, Boutros M, et al. Endothelial RSPO3 controls vascular stability and pruning through non-canonical WNT/Ca^{2+}/NFAT signaling. Dev Cell 2016;36:79–93.
23. Kabiri Z, Greicius G, Madan B, Biechele S, Zhong Z, Zaribafzadeh H, et al. Stroma provides an intestinal stem cell niche in the absence of epithelial Wnts. Development 2014;141:2206–15.
24. Gong X, Yi J, Carmon KS, Crumbley CA, Xiong W, Thomas A, et al. Aberrant RSPO3-LGR4 signaling in Keap1-deficient lung adenocarcinomas promotes tumor aggressiveness. Oncogene 2015;34:4692–701.
25. Chartier C, Raval J, Axelrod F, Bond C, Cain J, Dee-Hoskins C, et al. Therapeutic targeting of tumor-derived R-spondin attenuates beta-catenin signaling and tumorigenesis in multiple cancer types. Cancer Res 2016;76:713–23.
26. Gattelli A, Zimberlin MN, Meiss RP, Castilla LH, Kordon EC. Selection of early-occurring mutations dictates hormone-independent progression in mouse mammary tumor lines. J Virol 2006;80:11409–15.

27. Theodorou V, Kimm MA, Boer M, Wessels L, Theelen W, Jonkers J, et al. MMTV insertional mutagenesis identifies genes, gene families and pathways involved in mammary cancer. Nat Genet 2007;39: 759–69.
28. Berardi DE, Flumian C, Campodonico PB, Urtreger AJ, Diaz Bessone MI, Motter AN, et al. Myoepithelial and luminal breast cancer cells exhibit different responses to all-trans retinoic acid. Cell Oncol (Dordr) 2015;38: 289–305.
29. Prat A, Parker JS, Karginova O, Fan C, Livasy C, Herschkowitz JI, et al. Phenotypic and molecular characterization of the claudin-low intrinsic subtype of breast cancer. Breast Cancer Res 2010;12:R68.
30. Williams C, Helguero L, Edvardsson K, Haldosen LA, Gustafsson JA. Gene expression in murine mammary epithelial stem cell-like cells shows similarities to human breast cancer gene expression. Breast Cancer Res 2009;11:R26.
31. Korkaya H, Paulson A, Charafe-Jauffret E, Ginestier C, Brown M, Dutcher J, et al. Regulation of mammary stem/progenitor cells by PTEN/Akt/β-catenin signaling. PLoS Biol 2009;7:e1000121.
32. Livasy CA, Karaca G, Nanda R, Tretiakova MS, Olopade OI, Moore DT, et al. Phenotypic evaluation of the basal-like subtype of invasive breast carcinoma. Mod Pathol 2006;19:264–71.
33. Recouvreux MS, Grasso EN, Echeverria PC, Rocha-Viegas L, Castilla LH, Schere-Levy C, et al. RUNX1 and FOXP3 interplay regulates expression of breast cancer related genes. Oncotarget 2016;7:6552–65.
34. Blick T, Hugo H, Widodo E, Waltham M, Pinto C, Mani SA, et al. Epithelial mesenchymal transition traits in human breast cancer cell lines parallel the CD44hi/CD24lo/- stem cell phenotype in human breast cancer. J Mammary Gland Biol Neoplasia 2010;15:235–52.
35. Gilles C, Polette M, Mestdagt M, Nawrocki-Raby B, Ruggeri P, Birembaut P, et al. Transactivation of vimentin by β-catenin in human breast cancer cells. Cancer Res 2003;63:2658–64.
36. Cai C, Yu QC, Jiang W, Liu W, Song W, Yu H, et al. R-spondin1 is a novel hormone mediator for mammary stem cell self-renewal. Genes Dev 2014;28:2205–18.
37. DiMeo TA, Anderson K, Phadke P, Feng C, Perou CM, Naber S, et al. A novel lung metastasis signature links Wnt signaling with cancer cell self-renewal and epithelial-mesenchymal transition in basal-like breast cancer. Cancer Res 2009;69:5364–73.
38. Micalizzi DS, Farabaugh SM, Ford HL. Epithelial-mesenchymal transition in cancer: parallels between normal development and tumor progression. J Mammary Gland Biol Neoplasia 2010;15:117–34.
39. Cichon MA, Nelson CM, Radisky DC. Regulation of epithelial-mesenchymal transition in breast cancer cells by cell contact and adhesion. Cancer Informatics 2015;14(Suppl 3):1–13.
40. Nelson CM, VanDuijn MM, Inman JL, Fletcher DA, Bissell MJ. Tissue geometry determines sites of mammary branching morphogenesis in organotypic cultures. Science 2006;314:298.
41. Kouros-Mehr H, Werb Z. Candidate regulators of mammary branching morphogenesis identified by genome-wide transcript analysis. Dev Dyn 2006;235:3404–12.
42. Matsuda Y, Schlange T, Oakeley EJ, Boulay A, Hynes NE. WNT signaling enhances breast cancer cell motility and blockade of the WNT pathway by sFRP1 suppresses MDA-MB-231 xenograft growth. Breast Cancer Res 2009;11:R32.
43. Xu J, Prosperi JR, Choudhury N, Olopade OI, Goss KH. beta-Catenin is required for the tumorigenic behavior of triple-negative breast cancer cells. PLoS One 2015;10:e0117097.
44. Constantinou T, Baumann F, Lacher MD, Saurer S, Friis R, Dharmarajan A. SFRP-4 abrogates Wnt-3a-induced β-catenin and Akt/PKB signalling and reverses a Wnt-3a-imposed inhibition of in vitro mammary differentiation. J Mol Signal 2008;3:10.
45. Zhang M, Atkinson RL, Rosen JM. Selective targeting of radiation-resistant tumor-initiating cells. Proc Natl Acad Sci U S A 2010;107:3522–7.
46. Creighton CJ, Li X, Landis M, Dixon JM, Neumeister VM, Sjolund A, et al. Residual breast cancers after conventional therapy display mesenchymal as well as tumor-initiating features. Proc Natl Acad Sci U S A 2009;106:13820–5.
47. Vadnais C, Shooshtarizadeh P, Rajadurai CV, Lesurf R, Hulea L, Davoudi S, et al. Autocrine activation of the Wnt/beta-catenin pathway by CUX1 and GLIS1 in breast cancers. Biol Open 2014;3:937–46.
48. Khramtsov AI, Khramtsova GF, Tretiakova M, Huo D, Olopade OI, Goss KH. Wnt/β-catenin pathway activation is enriched in basal-like breast cancers and predicts poor outcome. Am J Pathol 2010;176:2911–20.
49. López-Knowles E, Zardawi SJ, McNeil CM, Millar EKA, Crea P, Musgrove EA, et al. Cytoplasmic localization of β-catenin is a marker of poor outcome in breast cancer patients. Cancer Epidemiol Biomarkers Prev 2010;19:301–9.
50. Geyer FC, Lacroix-Triki M, Savage K, Arnedos M, Lambros MB, MacKay A, et al. beta-Catenin pathway activation in breast cancer is associated with triple-negative phenotype but not with CTNNB1 mutation. Mod Pathol 2011;24:209–31.
51. Rooney N, Riggio AI, Mendoza-Villanueva D, Shore P, Cameron ER, Blyth K. Runx genes in breast cancer and the mammary lineage. In: Groner Y, Ito Y, Liu P, Neil JC, Speck NA, van Wijnen A, editors. RUNX proteins in development and cancer. Singapore: Springer; 2017, p. 353–68.
52. Pfefferle AD, Spike BT, Wahl GM, Perou CM. Luminal progenitor and fetal mammary stem cell expression features predict breast tumor response to neoadjuvant chemotherapy. Breast Cancer Res Treat 2015;149:425–37.

Published OnlineFirst May 10, 2018; DOI: 10.1158/0008-5472.CAN-17-2676

Cancer Research
The Journal of Cancer Research (1916–1930) | The American Journal of Cancer (1931–1940)

AACR American Association for Cancer Research

R-spondin3 Is Associated with Basal-Progenitor Behavior in Normal and Tumor Mammary Cells

Johanna M. Tocci, Carla M. Felcher, Martín E. García Solá, et al.

Cancer Res 2018;78:4497-4511. Published OnlineFirst May 10, 2018.